

## Experimental and Numerical Investigations on Multicellular GFRP Bridge Deck Panels

M. P. Muthuraj<sup>1,2</sup>, K. Nithyapriya<sup>1</sup>

**Abstract:** The maintenance, upgrading and replacement of existing bridges have become urgent requirement and a challenging task for the construction sector. Bridge decks made of fibre reinforced polymers (FRP), have been widely adopted both in new construction and replacement of existing bridge decks. This paper reports the studies carried out hand lay-up multicellular glass fibre reinforced polymer. Multicellular bridge deck panels with various cross sectional profiles have been analysed using a general purpose finite element software ANSYS. A cross sectional profile that satisfied the deflection criteria with minimum weight was selected for analysis and fabrication. Six multicellular GFRP composite bridge deck panel of size 1250mm × 333mm × 150mm ( $l \times b \times d$ ) were fabricated by hand lay-up process using various materials. The responses have been compared with analytical and numerical solutions and found to be they are in good agreement with each other.

**Keywords:** Glass fibre, bridge deck, finite element analysis, analytical, static

### 1 Introduction

In the present scenario, road authorities manage a large population of ageing bridges, a large number of which fail to meet the current requirements either due to deterioration and other structural deficiencies or as a result of the increasing demands imposed by increased traffic intensity and higher axle loads. As a result, the maintenance, upgrading and replacement of existing bridges have become a very difficult task for the construction sector. Due to the non-corrosive properties, fibre reinforced polymer (FRP) bars are being used as the replacement of steel reinforcement in concrete bridge deck slabs, which is an alternative solution to improve the service life of bridges [El-Gamal, El-Salakawy and Benmokrane (2005)]. Due to low elastic modulus of GFRP materials, GFRP reinforced sections exhibit higher deforma-

---

<sup>1</sup> Assistant Professor in Civil Engineering, Coimbatore Institute of Technology, Coimbatore, India-641 014

<sup>2</sup> Corresponding author. E-mail: m\_p\_muthuraj@rediffmail.com.

bility when compared to equivalent reinforced steel sections. Hence, the deflection criterion governs the design of intermediate and long spanning sections reinforced with GFRP bars [El-Salakawy, Benmokrane, El-Ragaby and Nadeau (2005); AASHTO (2000); ACI-440 (2008); CAN/CSA-S6-00 (2006)]. Bridge decks made of fiber reinforced polymers (FRP) have been widely studied and found to be increasingly used in highway bridges, both in new construction and replacement of existing bridge decks. FRP composite materials in general have a number of advantages including, high specific stiffness and specific strength ratios, increased fatigue behavior, and corrosion resistance. But compared to traditional construction materials, such as steel, timber, and concrete, GFRP has different material properties and structures made of GFRP found to exhibit specific behaviors [Qiao, Davalos and Brown (2000)]. Investigations on FRP bridge decks were conducted through laboratory tests on FRP deck components and field tests on FRP bridges [Shenton III and Chajes (1999); Turner, Harries, Petrou and Rizos (2004)]. Furthermore, it is known that parametric studies on experiment of various types are time consuming and expensive. Numerical simulations based on advanced methods, such as the finite element method (FEM), are reliable and cost effective alternatives in structural analysis for the study of structural response and performance. Finite Element analysis was successfully employed in research studying the performance of FRP bridge decks or their components [Davalos, Qiao, Xu, Robinson and Barth (2001); He and Aref (2003); Wu, Mu and Warnemuende (2003)].

Baolin et al. (2005) carried out numerical simulations for the GFRP bridge deck system and compared with the corresponding field response. The main parameters considered for the analysis include (i) developed FEM models (a) diaphragms, (b) girder stiffness, (c) girder spacing, (d) composite action and geometric and material nonlinearities. Alagusundaramoorthy and Reddy (2008) investigated the load – deflection behaviour of GFRP composite deck panels under static loading. Vovesny and Rotter (2012) carried out analysis and design of new bridge deck panel made of glass fiber reinforced polymer (GFRP). Zheng, Fu, Lu and Pan (2013) presented a numerical study of the structural behaviour of concrete bridge deck slabs under static patch loads and dynamic traffic loads and an investigation of compressive membrane action (CMA) inside slabs. Zhu and Lopez (2014) presented results obtained from experimental and analytical study of a newly developed lightweight composite bridge deck system composed of pultruded trapezoidal GFRP tubes and outer wrap. Flexural stiffness was evaluated and compared for panels with different grout materials and grouting patterns. From the analytical model, it was found that shear deformation must be considered for the accurate prediction of GFRP panels. Li, Badjie, Chen and Chiu (2014) discussed the features of the pedestrian bridge, detailed designs, a new method of digitally archiving the pedestrian bridge, theoret-

ical and FEM results. Mara, Haghani and Harryson (2014) examined the efficiency of GFRP system with traditional system and found that FRP decks contribute to potential cost savings over the life cycle of bridges and a reduced environmental impact. Ascione, Mancusi, Spadea, Lamberti, Lebon and Maurel-Pantel (2015) presented experimental results on the mechanical performance of composite beams obtained by bonding Glass Fibre Reinforced Polymer (GFRP) rectangular pultruded panels by means of an epoxy structural adhesive. No significant loss of performance in terms of failure load is observed but an increase of pre-failure stiffness was observed. Correia, Bai and Keller (2015) made a critical review on the fire performance of pultruded GFRP profiles. Review was made on several aspects such as fire performance of pultruded GFRP profiles, experimental and modelling studies about the fire resistance behaviour of different types of GFRP structural members and summary of the design guidance set out in the most relevant guidelines and codes applicable to pultruded GFRP structures.

Further, it is observed that the research investigations carried out on hand lay-up FRP composite bridge decks under static and fatigue behaviour of prototype decks are scanty. The main scope of the present investigation is to study experimental, analytical and numerical behaviour of hand lay-up multicellular GFRP composite bridge deck panels under static loading.

## 2 Materials and methods

Epoxy resins (ER) and ISO are chosen as resin Woven roving (WR) and Chopped strand mat (CSM) are chosen as matrix for the present study. Table 1 presents the various properties obtained for E-Glass fibre, ER and ISO. The properties include Modulus of elasticity, Volume fraction and Poisson’s ratio.

Table 1: Properties of E-Glass Fibre, ISO and ER

Properties	E-Glass Fibre	ISO	ER
Modulus of Elasticity, (N/mm <sup>2</sup> )	72400	3450	5000
Volume fraction, V	33.33%	66.67%	66.67%
Poisson’s ratio, $\gamma$	0.22	0.33	0.30

The properties of GFRP composites depend on the properties of material constituents (i.e., reinforcing fibre, matrix) and the corresponding volume fractions. Table 2 shows the material properties of the composite based on the properties of its constituents.

Preliminary analysis was carried out on various models created using general purpose finite element software ANSYS by applying Indian Road Congress (IRC)

Table 2: Material Properties of the E-Glass - Epoxy Composite

$E_x$ (GPa)	$E_y$ (GPa)	$G_{xy}$ (GPa)	$\nu_{xy}$	$\nu_{yx}$
27.467	7.250	3.44	0.293	0.077

class A loading to optimize the cross sectional profile that can be used for the fabrication of the experimental models. To obtain the maximum bending moment and shear force, the maximum wheel load was placed as shown in Figure 1. The ground contact area for the maximum axle load of 114 kN as specified in IRC 6 - 2000 is 500 mm perpendicular to the direction of motion and 250 mm parallel to the direction of motion. The minimum clearance was ensured between the outer edge of the wheel and the inner face of the kerb is 150 mm for all carriage way widths. The width of a single lane carriage way is 3.75 m and that of two lane carriage way is 7.5 m as per IRC 5 - 1998. The ground contact area for the maximum axle load and the distances between the wheels in both directions is indicated in Figure 1.

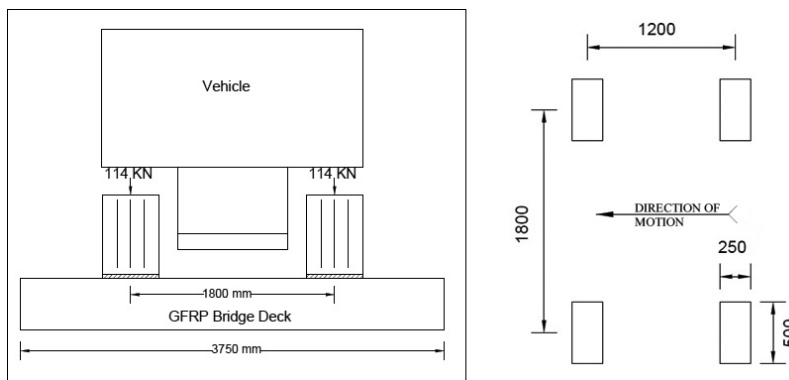


Figure 1: IRC Class A loading and ground contact area (All dimensions are in mm)

Various cross sectional profiles of multicellular bridge deck panels available in the literature were selected and analyzed for IRC Class A wheel load using ANSYS. The cross sections considered for FE analysis are shown in Figure 2. The overall dimensions are arrived at based on the Indian Roads Congress codes. The overall length of multicellular bridge deck panels were kept equal to the carriage way width of single lane, 3750 mm. and the width considered was 1000 mm.

SOLID45 brick elements were employed to model the bridge deck panel. SOLID45 element is defined by eight nodes having three degrees of freedom (translations in  $x$ ,  $y$  and  $z$ -directions) at each node with orthotropic material properties. Orthotropic

material directions correspond to the element coordinate directions. The bridge deck panel was assumed to be simply supported over two opposite edges.

The GFRP material is considered to have a linearly elastic behavior till failure. The Hooke’s law constitutive relations for orthotropic GFRP material used in the FEA are given in Eq. (1). Material properties provided in Table 1 and Table 2 for an orthotropic material were used in FEA. The parts were connected using a continuous mesh with shared common nodes and therefore a continuous stress is experienced between parts. Boundary conditions follow a simple support condition: a vertical displacement (in the y direction) and transverse displacement (x direction) restrain on the nodes of both ends; a z direction constraint at one of the ends.

$$\begin{Bmatrix} \varepsilon_z \\ \varepsilon_x \\ \varepsilon_y \\ \gamma_{xz} \\ \gamma_{yz} \\ \gamma_{xz} \end{Bmatrix} = \begin{bmatrix} \frac{1}{E_z} & -\frac{\nu_{xz}}{E_x} & -\frac{\nu_{yz}}{E_y} & 0 & 0 & 0 \\ -\frac{\nu_{xz}}{E_z} & \frac{1}{E_x} & -\frac{\nu_{xy}}{E_y} & 0 & 0 & 0 \\ -\frac{\nu_{yz}}{E_z} & -\frac{\nu_{xy}}{E_x} & \frac{1}{E_y} & 0 & 0 & 0 \\ 0 & 0 & 0 & \frac{1}{G_{xy}} & 0 & 0 \\ 0 & 0 & 0 & 0 & \frac{1}{G_{yz}} & 0 \\ 0 & 0 & 0 & 0 & 0 & \frac{1}{G_{xz}} \end{bmatrix} \begin{Bmatrix} \sigma_z \\ \sigma_x \\ \sigma_y \\ \tau_{xy} \\ \tau_{yz} \\ \tau_{xz} \end{Bmatrix} \quad (1)$$

where

$$\frac{\nu_{yx}}{E_y} = \frac{\nu_{xy}}{E_x}, \quad \frac{\nu_{zx}}{E_z} = \frac{\nu_{xz}}{E_x}, \quad \frac{\nu_{zy}}{E_z} = \frac{\nu_{yz}}{E_y} \quad (2)$$

In Eqs. (1) and (2), subscripts x, y and z correspond, respectively, to the transverse, the vertical, and the longitudinal directions of the GFRP girder. The initial  $\varepsilon$  stands for normal strain;  $\gamma$  stands for shear strain;  $\sigma$  is the normal stress;  $\tau$  is the shear stress;  $E$  is the Young’s Modulus;  $G$  is the shear modulus and  $\nu$  is the Poisson’s ratio.

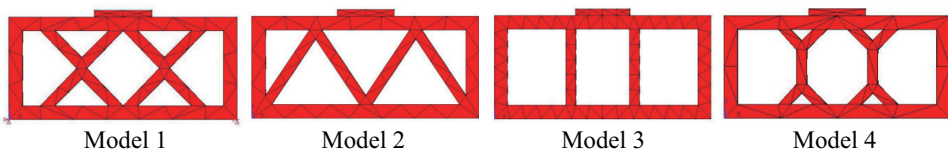


Figure 2: Cross sectional profiles considered for optimization

The depth and skin thickness of the cross section of bridge deck panels were varied by trial and error basis. IRC class A loading was imposed in the form of rectangular patch loads and the maximum deflection at the center of each panel under the factored load was obtained. The deflection values obtained for all the models is shown in Table 3. A cross sectional profile of the fourth model is satisfied the deflection criteria with minimum weight and is considered for further study. The analysis made on the cross sectional profile of the fourth model with varying thicknesses of flanges, webs and stiffeners is shown in Figure 3.

Table 3: Deflection (mm) values for various models

Model-1	Model-2	Model-3	Model-4	Model-5	Model-6	Model-7
6.50	5.64	2.49	2.34	3.3.4	2.84	2.34

FEA was performed for models 5, 6 and 7 and the deflection values obtained for these models are presented in Table 3. From Table 3, it can be noted that the lesser deflection is achieved for the geometry of model 7 and it is considered as model with optimum dimensions. The line diagram of optimised cross section is shown in Figure 4.

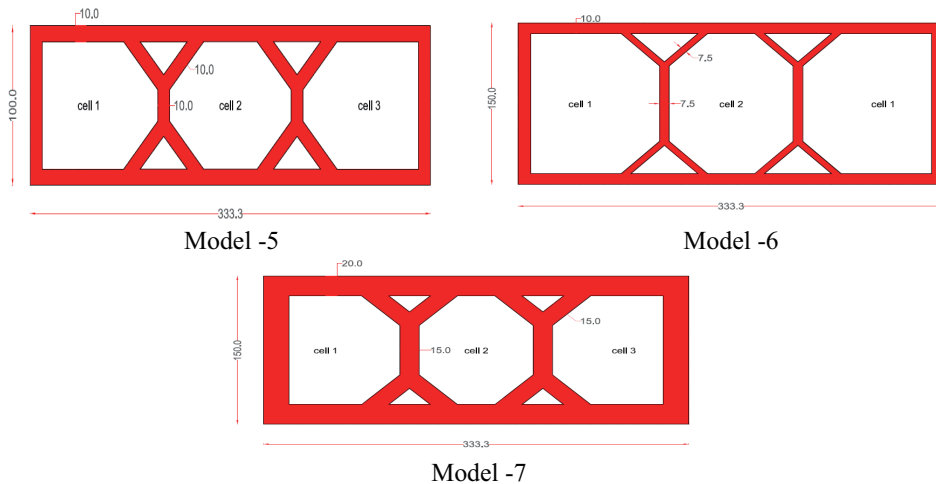


Figure 3: Cross sectional profiles with flange, web and stiffener thicknesses

The optimized cross section consists of a 3-cell section with additional stiffeners connecting the web to the top flange. The thickness of the top flange, bottom flange and the exterior webs are kept as 60 mm. The thickness of additional stiffeners

is kept as 45 mm. The experimental models used in this investigation are a 1:3 scale model of a 3.75m bridge superstructure. The dimensions of the prototype and one-third scaled model of the bridge deck panel are given in Table 4.

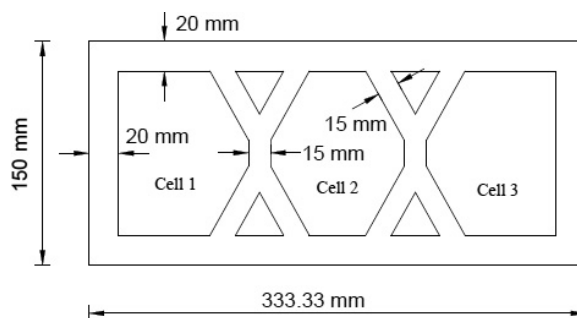


Figure 4: Cross sectional profile of one - third scaled model

Table 4: GFRP Bridge Deck Panel Dimensions

Parameter	Prototype (in mm)	Model (in mm)
Length	3750	1250
Width	1000	333.33
Depth	450	150
Flange and outer web thickness	60	20
Inner web thickness	60	15
Additional stiffeners	45	15

The GFRP bridge deck panel with the dimensions mentioned in Table 4 was analyzed by assigning the orthotropic material properties for the composites composed of the following materials.

- E-Glass fibres in the form of CSM and ISO
- E-Glass fibres in the form of WR and ISO
- E-Glass fibres in the form of WR and ER

The followings are notations for the six multi-cellular GFRP composite bridge considered for analysis.

1. CSIS1A - CSM and ISO under flexural loading condition

2. CSIS2A - CSM and ISO under shear loading condition
3. WRIS1A - WR and ISO under flexural loading condition
4. WRIS2A - WR and ISO under shear loading condition
5. WRER1A - WR and ER under flexural loading condition
6. WRER2A - WR and ER under Shear loading condition

The static analysis of multicellular GFRP composite bridge deck panel of size 1250 mm × 333.33 mm × 150 mm was carried out using ANSYS. Analysis is carried out for long edges simply supported and short edges simply supported as shown in Figure 5. The load was uniformly distributed over two rectangular patch areas of 166.67 mm × 83.33 mm up-to ultimate load on bridge deck panel in the form of equivalent nodal forces. Figure 5 shows the GFRP bridge deck FE model.

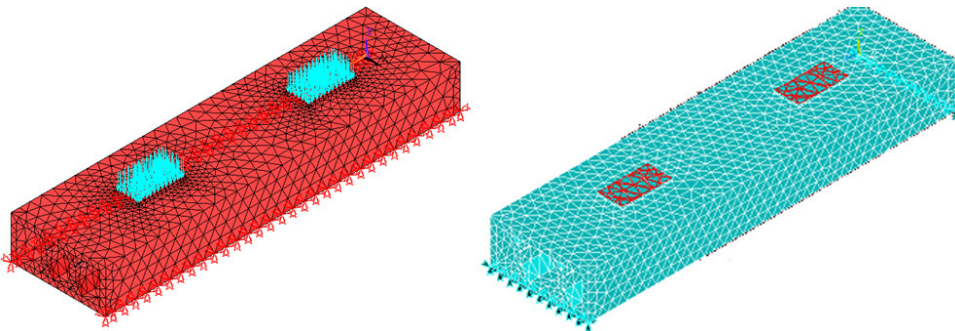


Figure 5: Finite element model with patch loads

The deflected shape of the deck panel under the load is shown in Figure 6 and the deflection contour of the bridge deck panel is shown in Figure 7 for WRIS2A and WRIS1A. Figure 8 shows the deflection contour of GFRP bridge deck panel made out of WRER2A and WRER1A in the case of two long edges and two short edges of simply supported condition.

The maximum deflection and ultimate load carrying capacity of three different models under flexure (short span hinged) and shear (long span hinged) conditions are presented in Table 5. From Table 5, it can be noted that the values of the maximum bending stress are found to be lower against maximum deflection.

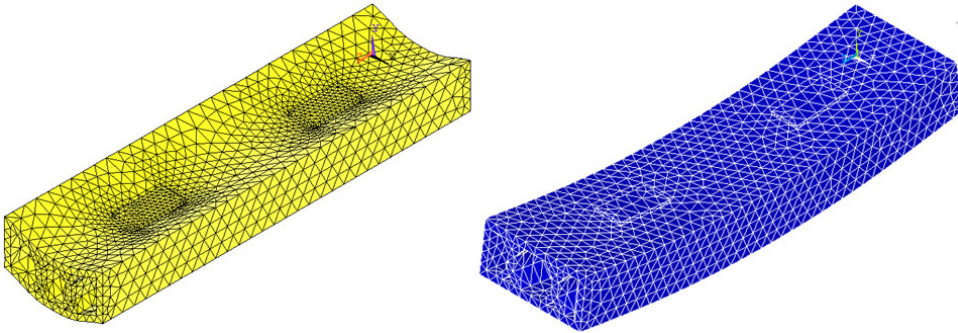


Figure 6: Deflected shape of the GFRP bridge deck panel (WRIS2A and WRIS1A)

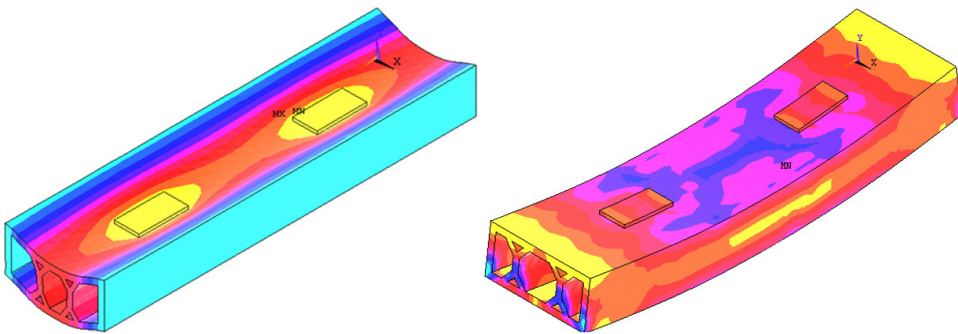


Figure 7: Deflection contour of the GFRP bridge deck panel (WRIS2A and WRIS1A)

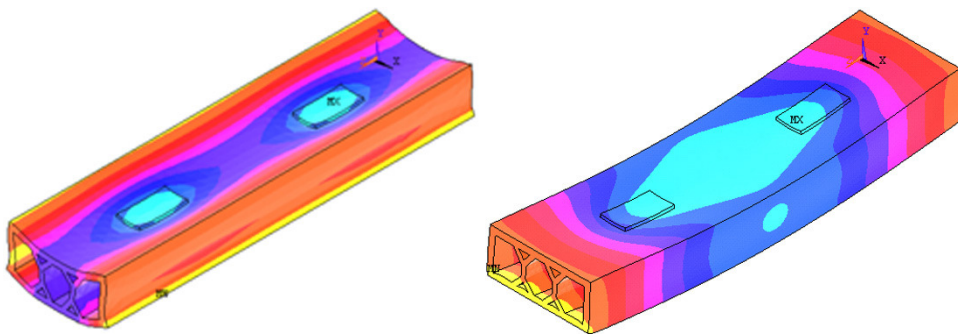


Figure 8: Deflection contour of the GFRP bridge deck panel (WRER2A and WRER1A)

### **3 Experimental investigations**

Three different combinations of materials were employed in the fabrication of the GFRP bridge deck panels as listed below.

Table 5: Ultimate Load and Maximum deflection

Models	Ultimate Load, kN	Maximum Deflection, mm	Maximum bending Stress, MPa
Flexure	CSIS1A	199.5	2.23
	WRIS1A	248.8	2.56
	WRER1A	264.2	2.34
Shear	CSIS2A	138.9	0.33
	WRIS2A	184.5	0.44
	WRER2A	246.8	0.38

- ISO and CSM made of E-glass.
- ISO and WR Mat 610 GSM made of E-glass
- ER and WR Mat (WRM) 610 GSM made of E-glass

Six multi-cellular GFRP composite bridge deck panels of size 1250 mm × 333 mm × 150 mm ( $l \times b \times d$ ) were fabricated by hand lay-up process using the following combination of materials.

- E-Glass fibres in the form of CSM and ISO – 2 Numbers
- E-Glass fibres in the form of WR and ISO – 2 Numbers
- E-Glass fibres in the form of WR and ER – 2 Numbers

Figure 9 shows typical bridge deck panel.

The loading frames were connected to the strong test floor. A Hydraulic jack was used for applying load. Proving ring of 300kN capacity was used for loading. Two points loading was applied on the model. The span length (1250 mm) of the bridge deck panel was kept parallel to the primary beam of the loading frame. The simply supported boundary conditions were simulated using the line supports as shown in Figure 9. The deflections were measured at the mid-span of the GFRP Deck panel and at the middle, inner and outer edges of the steel plates using the LVDT. The static testing of GFRP composite bridge deck panel was carried out under the simulated wheel load of IRC Class A wheeled vehicle. The dynamic allowance factor was taken as 30% of the live load of the wheeled vehicle. The static tests were conducted till failure.

While testing the bridge deck panel, no load shedding was observed even though the resin started cracking. A very little cracking sound was heard due to fracture of



Figure 9: Typical bridge deck panel

mat fabric inside the cells and also a loud cracking sound was heard as soon as the applied load reached the ultimate capacity of bridge deck panel and the specimen load shedding suddenly. The fracture of specimens proved its brittle nature. The rupture of fabric was found at the junctions of the triangular stiffeners (as shown in Figure 10) in all the three cells.

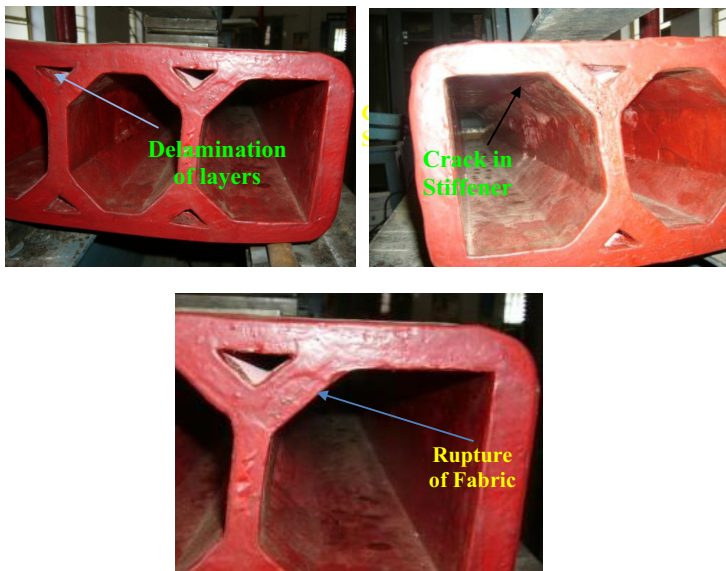


Figure 10: Failure pattern at the junctions of the triangular stiffeners

Table 6 presents the ultimate load and corresponding deflection obtained for all the GFRP bridge deck panels.

Table 6: Experimental ultimate load and deflection

Models	Ultimate Load, kN	Maximum deflection, mm
Flexure	CSIS1	202
	WRIS1	256
	WRER1	270
Shear	CSIS2	144
	WRIS2	191
	WRER2	255

From Tables 5 and 6, it can be noted that the computed ultimate load and corresponding deflections are in very good agreement with the corresponding experimental values. The developed FE models are found to be robust and reliable, which can be used for further parametric studies.

#### 4 Analytical studies

Analytical studies were carried out by using well known Euler Bernoulli beam theory (EBT) and Timeshenko Beam theory (TBT) to verify the experimental as well as FEA results. Table 7 presents the results of analytical studies.

Table 7: Analytical studies

Model	Deflection (mm) by	
	EBT	TBT
CSIS1A	2.21	2.26
WRIS1A	2.50	2.59
WRER1A	2.29	2.36

From Table 7, it can be noted that the deflections are in very good agreement with the corresponding FEA and experimental values.

#### 5 Summary

Experimental, numerical and analytical studies were carried out on hand lay-up prototype multicellular GFRP composite bridge deck panels. Linear static analysis has been carried out on various cross section profiles of GFRP bridge deck panel by using general purpose finite element software, ANSYS. Ultimate load and

corresponding deflections were obtained for all the cases. Based on the weight and minimum deflection, final configuration is arrived at. Bridge deck panels were fabricated by hand lay-up process and tested up to failure. Ultimate load and corresponding deflections were noted for each case. Deflections were also computed by Euler bending theory and Timoshenko beam theory. From the overall study it is observed that the deflections obtained by FEA, experiment and analytical are in very good agreement with each other. The developed FE model and analytical models are found to be robust and reliable.

## References

**AASHTO** (2000): *American Association of State Highway and Transportation Officials*. Standard specifications for design of highway bridges, Washington, DC, USA.

**ACI-440** (2008): *Guide for the design and construction of externally bonded FRP systems for strengthening concrete structures*. American Concrete Institute (ACI), Committee 440, Michigan, USA.

**Alagusundaramoorthy, P.; Reddy, R. V. S.** (2008): Testing and evaluation of gfrp composite deck panels. *Ocean Engineering*, vol. 35, no. 3, pp. 287–293.

**Ascione, F.; Mancusi, G.; Spadea, S.; Lamberti, M.; Lebon, F.; Maurel-Pantel, A.** (2015): On the flexural behaviour of gfrp beams obtained by bonding simple panels: An experimental investigation. *Composite Structures*, vol. 131, pp. 55–65.

**CAN/CSA-S6-00** (2006): *Canadian highway bridge design code*. Canadian Standards Association, Mississauga, ON, Canada.

**Correia, J. R.; Bai, Y.; Keller, T.** (2015): A review of the fire behaviour of pultruded gfrp structural profiles for civil engineering applications. *Composite Structures*, vol. 127, pp. 267–287.

**Davalos, J. F.; Qiao, P.; Xu, X. F.; Robinson, J.; Barth, K. E.** (2001): Modeling and characterization of fiber-reinforced plastic honeycomb sandwich panels for highway bridge applications. *Composite structures*, vol. 52, no. 3, pp. 441–452.

**El-Gamal, S.; El-Salakawy, E.; Benmokrane, B.** (2005): Behavior of concrete bridge deck slabs reinforced with fiber-reinforced polymer bars under concentrated loads. *ACI Structural Journal*, vol. 102, no. 5, pp. 727.

**El-Salakawy, E.; Benmokrane, B.; El-Ragaby, A.; Nadeau, D.** (2005): Field investigation on the first bridge deck slab reinforced with glass frp bars constructed in canada. *Journal of composites for construction*, vol. 9, no. 6, pp. 470–479.

**He, Y.; Aref, A. J.** (2003): An optimization design procedure for fiber reinforced polymer web-core sandwich bridge deck systems. *Composite Structures*, vol. 60, no. 2, pp. 183–195.

**Li, Y.-F.; Badjie, S.; Chen, W. W.; Chiu, Y.-T.** (2014): Case study of first all-grfp pedestrian bridge in taiwan. *Case Studies in Construction Materials*, vol. 1, pp. 83–95.

**Mara, V.; Haghani, R.; Harryson, P.** (2014): Bridge decks of fibre reinforced polymer (frp): a sustainable solution. *Construction and Building Materials*, vol. 50, pp. 190–199.

**Qiao, P.; Davalos, J. F.; Brown, B.** (2000): A systematic analysis and design approach for single-span frp deck/stringer bridges. *Composites Part B: Engineering*, vol. 31, no. 6, pp. 593–609.

**Shenton III, H. W.; Chajes, M. J.** (1999): Long-term health monitoring of an advanced polymer composite bridge. In *1999 Symposium on Smart Structures and Materials*, pp. 143–151. International Society for Optics and Photonics.

**Turner, M. K.; Harries, K. A.; Petrou, M. F.; Rizos, D.** (2004): In situ structural evaluation of a grfp bridge deck system. *Composite Structures*, vol. 65, no. 2, pp. 157–165.

**Vovesnỳ, M.; Rotter, T.** (2012): Gfrp bridge deck panel. *Procedia Engineering*, vol. 40, pp. 492–497.

**Wu, H.-C.; Mu, B.; Warnemuende, K.** (2003): Failure analysis of frp sandwich bus panels by finite element method. *Composites Part B: Engineering*, vol. 34, no. 1, pp. 51–58.

**Zheng, Y.; Fu, X.; Lu, Z.; Pan, Y.** (2013): Investigation of structural behaviour of grfp reinforced concrete deck slabs through nlfea. *Construction and Building Materials*, vol. 45, pp. 60–77.

**Zhu, J.; Lopez, M. M.** (2014): Performance of a lightweight grfp composite bridge deck in positive and negative bending regions. *Composite Structures*, vol. 113, pp. 108–117.